Articles

Mapping the Binding Site of P53 on UBC9 by NMR Spectroscopy

LIN, Dong-Hai[*,a,b](林东海)

[a] *Department of Biochemistry, The Hong Kong University of Science & Technology, Hong Kong, China*

[b] *Center for Drug Discovery and Design, State Key Laboratory of Drug Research, Shanghai Institute of Meteria Medica, Shanghai Institutes of Biological Sciences, Chinese Academy of Sciences, Shanghai 200031, China*

Human UBC9 is a member of the E2 family of proteins. However, instead of conjugating to ubiquitin, it conjugates to a ubiquitin homologue SUMO-1 (also known as UBL1, GMP1, SMTP3, PICT-1 and sentrin). The SUMO-1 conjugation pathway is very similar to that of ubiquitin with regard to the primary sequences of the ubiquitin activating enzymes (E1), the three-dimensional structures of the ubiquitin conjugating enzymes (E2), and the chemistry of the overall conjugation pathway. The interaction of p53 and UBC9, the E2 of the SUMO-1 pathway, has been studied by nuclear magnetic resonance spectroscopy. A peptide corresponding to the nuclear localization domain of p53 specifically interacts with UBC9 and this interaction is likely to be important for conjugation of p53 with SUMO-1. The largest chemical shift changes on UBC9 occur at residues 94 and 129—135. This region is adjacent to the active site and has significant dynamic behavior on the μs—ms and ps—ns timescales. Correlation of chemical shift changes and mobility of these residues further suggest the importance of these residues in substrate recognition.

Keywords NMR, protein-peptide interaction, SUMO-1 pathway, E2 enzyme, p53

Introduction

SUMO-1 (also known as UBL1, GMP1, SMTP3, PICT-1 and sentrin) is a ubiquitin homologue, and has been shown to play important roles in cellular functions such as DNA-repair and p53 dependent processes.[1] The SUMO-1 conjugation pathway is very similar to that of ubiquitin with regard to the primary sequences of the ubiquitin activating enzymes (E1), the three-dimensional structures of the ubiquitin conjugating enzymes (E2), and the chemistry of the overall conjugation pathway. Similar to the ubiquitin pathway, the C-terminal Gly residue of SUMO-1 is involved in covalent conjugation to a Lys residue of other proteins. In the ubiquitin pathway, ubiquitin is first activated by an enzyme E1 through hydrolysis of ATP to form a high energy bond between the C-terminal Gly residue of ubiquitin and a Cys residue in E1. Then, ubiquitin is transferred to a ubiquitin conjugation enzyme (UBC) known as E2. In this step, the C-terminal Gly of ubiquitin is conjugated to the SH group of the active site Cys residue of E2. The E2 interacts with substrate proteins to transfer ubiquitin to the substrate proteins.

E2 enzymes in the ubiquitination and homologous pathways catalyze the conjugation of ubiquitin or its homologues with target proteins, and therefore are likely to play important roles in target protein recognition. Although it has been proposed that E2 can interact with target proteins, the binding site of target proteins on E2 is still not clear. The three-dimensional structures of human UBC9 and several other E2 proteins have been determined.[3-7] In addition, conformational flexibility of UBC9 has been characterized by NMR methods.[8] E2 enzymes have a highly conserved three-dimensional structure. UBC9 has an overall rigid conformation, but several regions have higher flexibility than that of average. In particular, a few residues near the active site have high mo-

* E-mail: donghail@ust.hk; Tel.: 852-23588785; Fax: 852-23581716

Received June 14, 2002; revised July 28, 2002; accepted August 5, 2002.

Project supported by the National Natural Science Foundation of China (No. 19975038).

bility on the μs—ms and ps—ns timesscales. These residues were proposed to play a role in target protein recognition or catalytic activity.

The modification of the tumor suppressor protein p53 by the SUMO-1 pathway has been well characterized.[9,10] Conjugation of p53 with SUMO-1 significantly increases the activity of p53 in the cells. It has been recently reported that conjugation of SUMO-1 to p53 occurs at Lys^{386} of p53. Lys^{386} is located in the nuclear localization domain. Deletion of the C-terminal 30 amino acid residues of p53 abolished the conjugation activity. We have examined the interactions of the nuclear localization domain of p53 and the SUMO-1 conjugation enzyme UBC9. The regions on UBC9 that is likely to form specific interactions with p53 have been mapped by chemical shift perturbation.

Materials and methods

Protein expression and purification

Human UBC9 was subcloned into vector PET28 as described previously.[8] The modified plasmids have an open reading frame that includes 6 His residues as an affinity tag at the N terminus followed by the sequence of UBC9. *Escherichia coli* cells containing the expression plasmid were grown at 37 ℃ in M-9 minimal media containing kanamycin (30 $g \cdot L^{-1}$) supplemented with trace minerals and basal medium Eagle vitamins. $^{15}NH_4Cl$ (1 $g \cdot L^{-1}$) and/or ^{13}C-glucose (2 $g \cdot L^{-1}$) were used as the only nitrogen and carbon sources for ^{15}N and/or ^{13}C-labeling.

Expression of the protein was induced by addition of IPTG (isopropyl β-*D*-thiogalactopyranoside) to a concentration of 1.0 $mmol \cdot L^{-1}$ when the cells had grown to an OD (at 595 nm) of 0.6—0.8. Cells were harvested three to four hours after induction and stored at −70 ℃. Then the cell pellets were suspended in buffer A (5 $mmol \cdot L^{-1}$ imidazole, 500 $mmol \cdot L^{-1}$ NaCl, 20 $mmol \cdot L^{-1}$ Tris-HCl, pH 7.9). The protein was extracted by sonication and centrifugation at 16500 r/min for 50 min.

The protein was purified on a column packed with Ni-NTA resin (Qiagen). The eluted proteins were concentrated and exchanged to a NMR buffer (100 $mmol \cdot L^{-1}$ sodium phosphate, pH 6.0, 0.02% NaN_3, 5 $mmol \cdot L^{-1}$ DDT, in 90% H_2O/10% D_2O). The purity of the protein was confirmed by SDS-polyacrylamide gel electrophoresis. Concentration of the protein was estimated with the Bio-Rad protein assay and 1 D proton NMR spectra.

The p53 peptide was synthesized by solid phase synthesis in the Peptide and Nucleic Acid Synthesis Facility of the City of Hope National Medical Center, USA. The peptide corresponds to the nuclear localization domain of p53, containing the last 30 amino acid residues of p53: AHSSHLKSKKGQSTSRHKKLMFKTEGPDSD. The peptide was dissolved in the same NMR buffer at concentrations of 10 $mmol \cdot L^{-1}$ and 33 $mmol \cdot L^{-1}$ at pH 6.0.

NMR *measurements*

All NMR spectra were acquired on a Varian UNITY-plus 500 MHz NMR spectrometer equipped with four channels, pulse shaping, *z*-axis pulsed field gradient capabilities. Titration of the p53 peptide to UBC9 was performed as follows. A sample of 0.7 $mmol \cdot L^{-1}$ ^{15}N-labeled UBC9 was titrated with 10 $mmol \cdot L^{-1}$ p53 peptide to molar ratios of 1:0.5, 1:1, 1:1.5, 1:2.0, 1:2.4, 1:2.9, 1:3.5 and 1:3.9. Additional titration experiments were performed with a 33 $mmol \cdot L^{-1}$ p53 stock solution to molar ratios of 1:8.7, 1:13.6 and 1:18.4. The backbone resonance assignments for human UBC9 have been described previously.[11] At each titration point, 2 D ^{15}N-^1H HSQC spectra[12] were recorded for bound ^{15}N-labeled UBC9. The spectral widths in the HSQC experiments were 1300 Hz in F_1 and 6000 Hz in F_2 dimensions with 128 and 512 complex points in the F_1 and F_2 dimensions, respectively. Linear prediction in the indirect dimension and zero-filling in both dimensions were used before Fourier transformation.

Determination of the dissociation constant K_d

For protein-peptide interaction, when exchange between the free state and the bound state is very fast with respect to the differences in chemical shifts between two states, a single resonance is observed (δ_{obs}) for a specific amide, which is the population-weighted average of the amide chemical shifts of the free state (δ_f) and bound state (δ_c). Under this condition, the following Eq. (1) can be deduced in a similar way used by Lian *et al*.[13]

$$\delta_{obs} - \delta_f = \frac{(\delta_c - \delta_f)}{2}\left\{1 + \frac{K_d}{[E]_0}\left(1 + \frac{V_i}{V_0}\right) + \frac{[S]_a}{[E]_0}\frac{V_i}{V_0} - \sqrt{\left[1 + \frac{K_d}{[E]_0}\left(1 + \frac{V_i}{V_0}\right) + \frac{[S]_a}{[E]_0}\frac{V_i}{V_0}\right]^2 - 4\frac{[S]_a}{[E]_0}\frac{V_i}{V_0}}\right\} \quad (1)$$

in which, $[E]_0$ and V_0 are the concentration and volume of the initial protein solution, respectively; $[S]_a$ and V_i are the concentration and volume of the peptide stock solution added during the titration, respectively. The dissociation constant K_d was determined by fitting Eq. (1) to experimental data.

Calculations of electrostatic potentials

The surface electrostatic potentials for UBC9 was calculated using the Delphi module of INSIGHT II (MSL, Inc.) and the crystal structure.[3] The solvent dielectric constant was set to 80. The radius of the probe water molecule was 1.4. The grids in the calculation of the electrostatic potentials were with a spacing of 1.5.

Results and discussion

The nuclear localization domain of p53 interacts with UBC9. It has been shown that p53 is modified by SUMO-1 at Lys^{386} in the nuclear localization domain and this modification is independent of the overall structural integrity of p53.[9,10] Therefore, chemical shift perturbation was used to detect whether a peptide corresponding to the nuclear localization domain of p53 specifically interacts with UBC9. Chemical shift perturbation is extremely sensitive to molecular interactions and has been widely used to map binding surfaces. In drug screening, it is employed to identify molecules that bind to a protein target, which is known as "SAR (Structure Activity Relationship) by NMR".[14]

^{15}N-labeled UBC9 and unlabeled p53 peptide were used for this study. ^{15}N-^{1}H HSQC selectively observes signals from UBC9 in the complex with p53. Specific chemical shift perturbation and changes in the linewidths were observed in ^{15}N-^{1}H HSQC spectra of UBC9 upon forming complex with the p53 peptide. These changes were consistent from the beginning of the titration, when the concentration of UBC9 was approximately 0.7 mmol·L^{-1} and that of the p53 peptide was 0.3 mmol·L^{-1}, until the final concentrations of the p53 peptide and UBC9 reached approximately 2.3 and 0.6 mmol·L^{-1}, respectively. Superposition of the HSQC spectra of free UBC9 and that in complex with the p53 peptide is shown in Fig. 1A. The plot of chemical shift changes versus residue number is shown in Fig. 1B. Most peaks of UBC9 were not affected, indicating that the complex formation does not cause large conformational changes in UBC9.

The largest chemical shift change occurs at residue Ala^{129}. This residue and the two sequentially connected residues (Pro^{128} and Gln^{130}) are conserved between the human and yeast UBC9. The sidechain of Ala^{129} approaches the sidechain of the conjugation active site Cys^{93} and the two sidechains are less than 0.5 nm apart. All observable residues between residues 129 and 135 show chemical shift changes larger than twice the digital resolution (0.01 ppm in the proton dimension or 0.05 ppm in the nitrogen dimension). In addition, residues Val^{92}, Leu^{94}, Gln^{126} (next to the conjugation active site Cys^{93}) and Val^{148} (next to the segment composed of residues 129—135 in the structure) is also affected significantly by binding of the p53 peptide. These residues are colored in red in the ribbon diagram of the UBC9 structure (Fig. 2A). Because these residues are close to each other in the three-dimensional structure and are adjacent to the conjugation active site, they are likely to form specific interactions with the p53 peptide. This segment contains mostly hydrophobic and polar residues, and has an overall neutral to slightly positive surface electrostatic potential (Fig. 2B). This region may be involved in hydrophobic interactions and hydrogen bonding with the p53 peptide and contribute to the specificity of the interaction. Additionally, local conformational changes due to p53 binding may also contribute to specific chemical shift changes of some of these residues.

In addition to the localized area of chemical shift changes, several other residues also show significant chemical shift changes and are indicated in gold in Fig. 2A. These residues are located between the active site Cys^{93} and the N-terminus in the three-dimensional structure. The chemical shift changes of all the residues indicated in gold in Fig. 2A are consistent with addition of the p53 peptide. These residues are not close to each other in the three-dimensional structure and the chemical shift changes are generally small. This surface has a strong negative electrostatic potential, as shown in Fig. 2B. Like many nuclear localization domains, the nuclear localization domain of p53 has an overall positive electro-

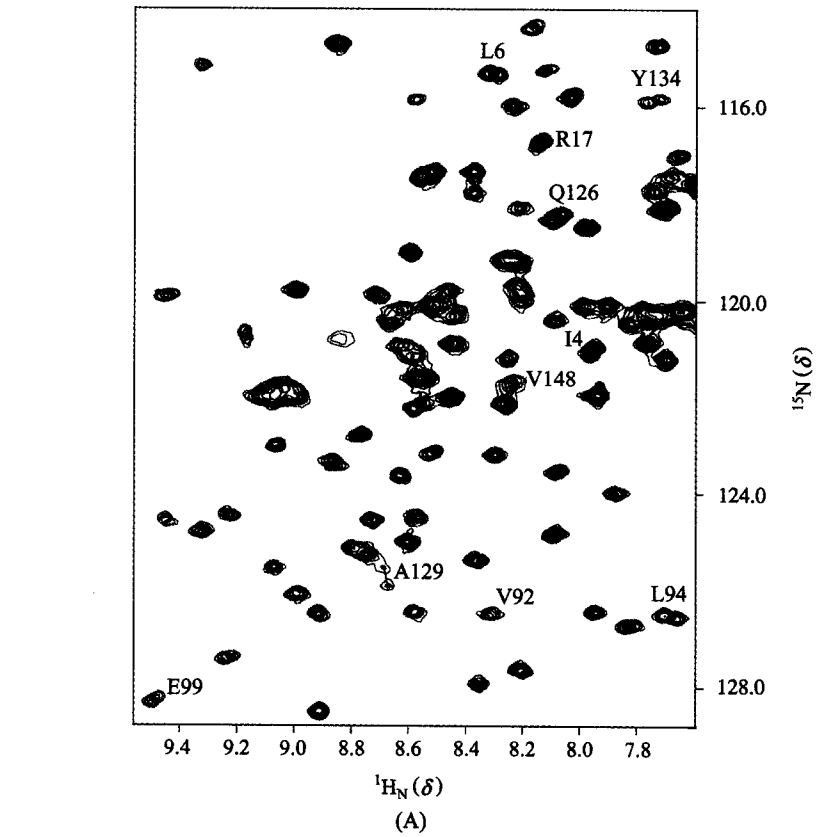

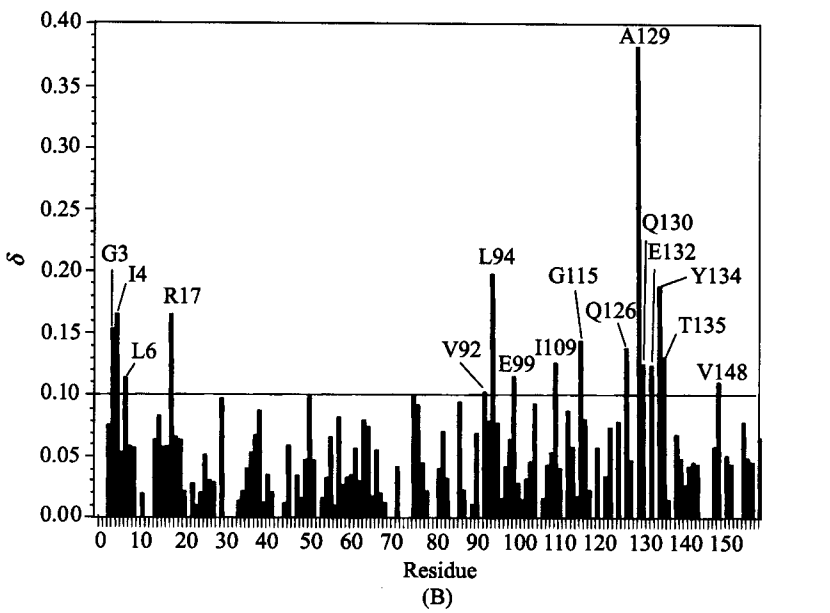

Fig. 1 (A) Superposition of a region of the ^{15}N -^{1}H HSQC spectra of ^{15}N-labeled UBC9, free (red) and in the complex with unlabeled p53 peptide (green). The molar ratio of p53 to UBC9 is 3.8:1. Only peaks affected significantly upon complex formation are indicated with their assignments. (B) Average chemical shift changes versus residue number of the ^{15}N-labeled UBC9 upon complex formation with the p53 peptide. The average chemical shift changes of peaks are calculated as $[(5\Delta\delta_{HN})^2 + (\Delta\delta_N)^2]^{1/2}$ where $\Delta\delta_{HN}$ represents the chemical shift change of the amide proton and $\Delta\delta_N$ represents the chemical shift change of the amide nitrogen of an amino acid residue.

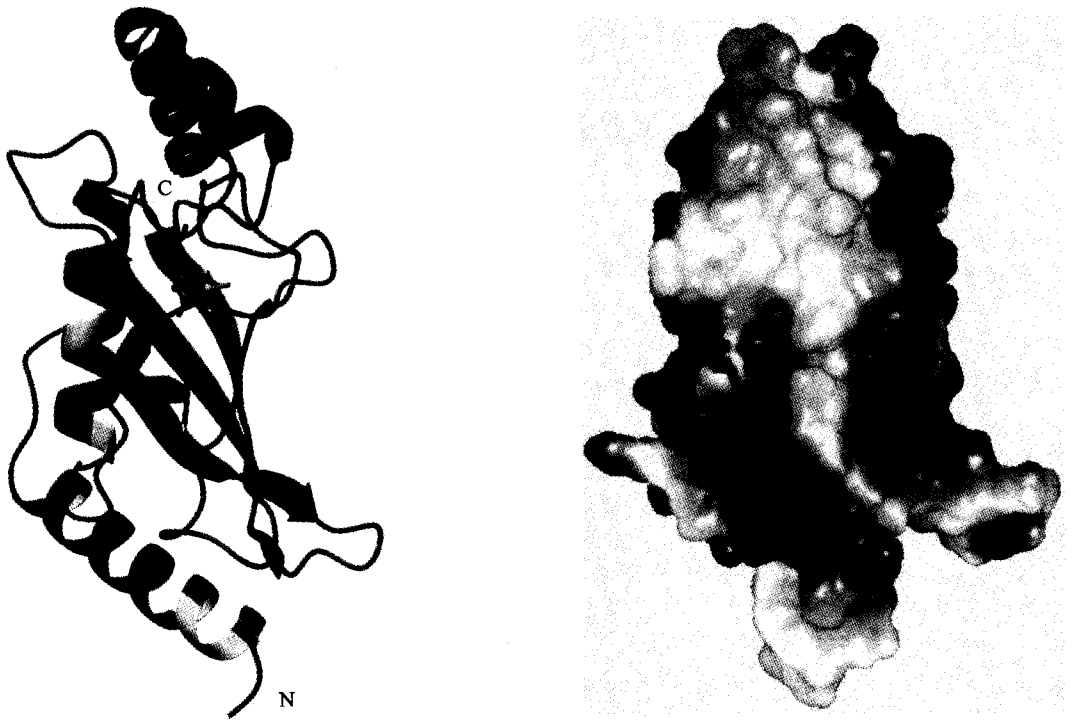

(A) (B)

Fig. 2 (A) Ribbon diagram of the three-dimensional structure of human UBC9. Chemical shift perturbations upon binding of the p53 peptide are indicated by the coloring scheme described in the text. The active site Cys^{93} is shown with its sidechain. (B) Surface electrostatic potentials of human UBC9. The orientation of the molecule is the same as that in (A). The charge topology was calculated and displayed using INSIGHT II (MSI, Inc.). The color spectrum from red to blue corresponds to changes from negative to positive potentials over a range of −5 to +5 KB/e.

static potential. The opposite electrostatic potentials between the p53 peptide and this surface on UBC9 suggest that electrostatic interactions may occur. Electrostatic interactions are generally long range and not highly specific, and may generate the pattern of chemical shift changes observed in these residues.

The dissociation constant K_d was estimated using the resonance of Ala^{129}, where the largest chemical shift change was observed. Fig. 3 shows the plot of ^{15}N chemical shift changes with increasing amounts of the p53 peptide. Using Eq. (1), the dissociation constant was estimated to be (4.7 ± 1.0) mmol·L^{-1}. Based on this dissociation constant, when the molar ratio of the p53 peptide to UBC9 is approximately 3.9 : 1.0, only approximately 34% of UBC9 is in the complex with p53, and the rest of the UBC9 molecules still are in free form. This is partly responsible for the small chemical shift changes observed. In order to induce maximum shifts in UBC9, three additional HSQC spectra were acquired by titration

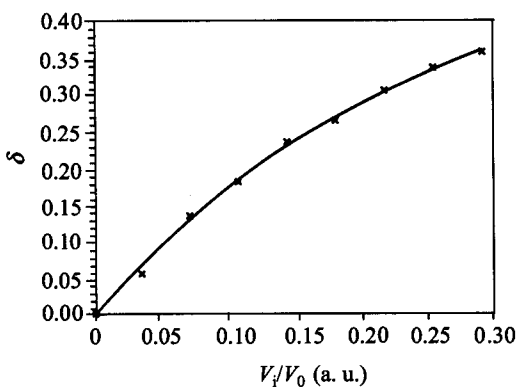

Fig. 3 Plot of ^{15}N chemical shift changes of Ala^{129} of UBC9 with increasing amounts of the p53 peptide. V_i is the volume of the p53 stock solution added to the UBC9 solution, and V_0 is the initial volume of the UBC9 sample. The dissociation constant K_d was estimated by fitting these titration points to Eq. (1) in the materials and methods section. The theoretical curve is shown as a solid line.

with a more concentrated p53 stock solution reaching relative molar ratios of the p53 peptide to UBC9 of 8.7:1, 13.6:1 and 18.4:1. It is estimated that approximately 68% of UBC9 were in the complex at the end of this titration. The residue that presented the most significant chemical shift changes was also Ala^{129}, and the relative chemical shift perturbations increased as expected. However, at these high concentrations of the p53 peptide, some residues that are not around the active site show inconsistent and random changes in chemical shifts. This suggests that some interactions are non-specific or not first-order at such high concentrations in these regions. In addition, significant protein precipitation occurred. Therefore the last three titrations were not used for detailed analysis.

The affinity between the p53 peptide and UBC9 is not likely to represent the affinity of p53 to the UBC9-SUMO-1 conjugate. In the SUMO-1 pathway, SUMO-1 first conjugates to UBC9, and then the UBC9-SUMO-1 conjugate interacts with target proteins to transfer SUMO-1 to the target proteins. SUMO-1 also specifically interacts with p53 (data not shown). Thus the affinity constant between the UBC9-SUMO-1 conjugate and the p53 peptide can be a few orders of magnitude higher due to the conjugation between UBC9 and SUMO-1.

Dynamics and substrate recognition

The residues that show significant chemical shift perturbation around the active site are located in the area of the highest conformational flexibility on the μs—ms timescale and significant dynamic behavior on the ps—ns timescale in UBC9.[8] The following residues near the active site Cys^{93} have higher conformational flexibility than average residues in the ps—ns and μs—ms timescale: Leu^{81}, Val^{86}, Ser^{89}, Val^{92}, Leu^{97}, Leu^{119}, Gln^{126}, Asp^{127}, Ala^{129}, Gln^{130} and Glu^{132}. Among these residues Val^{86}, Val^{92}, Leu^{97}, Leu^{119}, Ala^{129}, and Glu^{132} have the highest flexibility on the μs—ms timescale ($R_{ex} > 4$ s) in UBC9. In particular, Glu^{132} has the largest R_{ex} term of the entire molecule (14.7 s^{-1}). Thus the region on UBC9 that has the most significant and localized chemical shift changes (residues 92, 94, 126, 129—135 and 148) upon complex formation with p53 has significant flexibility on the ps—ns and μs—ms timescales.

Although three-dimensional structures of proteins and their complexes provide significant insights into the determinants of binding affinity and specificity, dynamics clearly plays important roles in molecular recognition and enzyme activities.[15,16] The flexible regions at the interface usually become more rigid upon complex formation. This induced structural formation is likely to be important for binding specificity, because non-specific interactions are unable to generate such "induced fits". In addition, changes in flexibility should modulate the affinity of the interaction through changes in entropy and its contribution to free energy changes. The correlation between chemical shift changes and dynamics of residues near the active site further suggests the importance of these residues in substrate recognition.

The substrate binding site on UBC9 identified in this study is consistent with previous studies. It has been suggested that the substrate binding site on a E2 enzyme is likely to be close to the C-terminus, because the E2 enzymes that have C-terminal extensions in the ubiquitination pathway do not require E3 for target protein recognition, while E2 enzymes that do not contain C-terminal extensions generally require E3.[2] The p53 binding site on UBC9 that has been identified in this study is close to the C-terminus of the molecule. In addition, some E2 enzymes contain insertions of variable lengths in a loop located at approximately residue Glu^{99} of UBC9. Because of the diversity in the sequences and lengths of the insertions among different E2 enzymes, this loop has been proposed to play a role in substrate specificity.[6] Chemical shift changes of some residues in this loop of UBC9 (Leu^{94} and Glu^{99}) have been observed. This loop is adjacent to the substrate binding site on UBC9 identified by chemical shift changes. Since the E2 proteins share a highly conserved three-dimensional structure, the binding site identified by chemical shift changes in this study may be involved in target protein recognition in the SUMO-1 pathway and perhaps ubiquitination pathways in general.

Acknowledgments

This work is supported in part by grants from the National Natural Science Foundation of China (No. 19975038) to D. Lin. and NIH GM59887 to Y. Chen. The author would like to thank Dr. Y. Chen for many useful discussions and helps.

References

1 Seufert, W.; Futcher, B.; Jentsch, S. *Nature* **1995**, *373*, 78.

2 Jentsch, S. *Annu. Rev. Genn.* **1992**, *26*, 179.

3 Tong, H.; Hateboer, G.; Perrakis, A.; Bernards, R.; Sixma, T. K. *J. Biol. Chem.* **1997**, *272*, 21381.

4 Cook, W. J.; Jeffrey, L. C.; Sullivan, M. L.; Vierstra, R. D. *J. Biol. Chem.* **1992**, *267*, 15116.

5 Cook, W. J.; Jeffrey, L. C.; Xu, Y.; Chau, V. *Biochemistry* **1993**, *32*, 13809.

6 Cook, W. J.; Martin, P. D.; Edwards, B. F. P.; Yamazaki, R. K.; Chau, V. *Biochemistry* **1997**, *36*, 1621.

7 Worthylake, D. K.; Prakash, S.; Prakash, L.; Hill, C. P. *J. Biol. Chem.* **1998**, *273*, 6271.

8 Liu, Q.; Yuan, Y.; Shen, B.; Chen, D. J.; Chen, Y. *Biochemistry* **1998**, *38*, 1415.

9 Rodriguez, M. S.; Desterro, J. M. P.; Lain, S.; Midgley, C. A.; Lane, D. P.; Hay, R. T. *EMBO J.* **1999**, 18, 6455.

10 Gostissa, M.; Hengstermann, A.; Fogal, V.; Sandy, P.; Schwarz, S. E.; Scheffner, M.; Sal, G. D. *EMBO J.* **1999**, *18*, 6462.

11 Liu, Q.; Shen, B.; Chen, D. J.; Chen, Y. *J. Biol. NMR* **1998**, *13*, 89.

12 Kay, L. E.; Keifer, P.; Saarinen, T. *J. Am. Chem. Soc.* **1992**, *114*, 10663.

13 Lian, L. Y.; Robert, G. C. K. In *NMR of Macromolecules——A Practical Approach*, Ed.: Robert. G. C. K., Oxford University Press, Oxford, **1993**, p. 154.

14 Shuker, S. B.; Hajduk, P. J.; Meadows, R. P.; Fesik, S. W. *Science* **1996**, *274*, 1531.

15 Spolar, R. S.; Record, M. T., Jr. *Science* **1994**, *263*, 777.

16 Wright, P. E.; Dyson, H. J. *J. Mol. Biol.* **1999**, *293*, 321.

(E0206145 ZHAO, X. J.)